AN EXPERIMENTAL STUDY OF FLAME KERNEL DEVELOPMENT AT DIFFERENT SPARK ENERGIES USING NEW DETECTION SYSTEMS

Diploma paper by

Mats Lindelöw

and

Hans Sturesson

Lund Reports on Atomic Physics, LRAP-103

Lund, June 1989

CONTENTS PAGE

1. ABSTRACT

Two different detection systems, one fibre-optic and the other using the technique of ionization probes, were used in the study of flame propagation rates. A coupling between the flame front propagation rate and the energy dissipated in the spark from a spark plug, particularly the first part of the energy (0-1 μs after the breakdown) was found. In order to vary the energy as much as possible, both a commercial capacitive system and an ultra-fast capacitive system were exploited. They were connected in turn to a coaxial and a conventional spark-plug. The experiments were performed in a static system, consisting of a high-pressure bomb filled with a stagnant propane-air gas mixture (4.1 % propane) at 0.4 MPa and room temperature.

2. INTRODUCTION

Internal combustion (I.C.) engines suffer from cycle-to-cycle variation of the indicated mean effective pressure, IMEP. This causes unnecessary wear of the mechanical parts, uneven power output and low efficiency. The variation is particularly severe when the burning rate is low, e.g. in cold starts or partial throttle acceleration, when the fuel flow cannot accelerate as quickly as the air flow. Also with lean mixtures, currently of great interest, the effect is troublesome. There are two ways of bringing IMEP variation within tolerable levels; to decrease the coupling between combustion and the IMEP, which requires substantial redesign of the engine, or to reduce the variations in the combustion process.

Fundamental importance of initial flame propagation rate

One important parameter in the combustion is the initial flame propagation rate. Variations in this rate constitute the major cause of cycle-by-cycle pressure variations (Refs 1,2,3). It is predicted in models (Refs 4,5,6), and is supported experimentally (Ref.7), that if the initial flame propagation rate is increased, the coupling between variations in flame rate and variations in pressure is decreased. This increase of flame propagation rate can be achieved by, for example using different fuels, richer mixtures or reducing the exhaust residual mass fraction, though none of these methods are practical in commercial engines. Instead much effort is being devoted to the investigation of ignition, as the flame propagation rate is highly dependent on this phase. Several different devices have been proposed such as plasma jets, torch cells and laser ignition, all reviewed by Dale and Oppenheim in 1981 (Ref.8). However, of the most practical interest in the immediate future is still the traditional spark ignition system.

Effects of long discharges

Previous work in this field has been mainly concerned with the minimum energy required to ignite the gas, and its dependence on various parameters. It was found by Rose & Priede (Ref.9) that the minimum energy is decreased if the spark duration is prolonged, so-called long discharges, and is also dependent on the breakdown voltage and the diameter of the spark plasma (Ref.10). Kono et al. (Ref.11) reported the optimum spark duration to be 50-300 μs. The narrower the gap, the thicker electrodes and the leaner the mixture, the longer the optimum spark duration, which is supported by experiments (Ref.12,13,14,15). Especially near the lean limit, long discharges are said to suppress misfires. A commercial system for producing long discharges (milliseconds) has been presented by Nissan (Ref.16), which is said to exhibitappreciable improvements in idling stability, acceleration and economy. One problem with long discharges though, has been the erosion of the electrodes.

Two effects influence electrode erosion. Pits are formed when electrons pass through the surface of the electrode; a process which is enhanced by the large current of the short discharge. The opposite effect in short discharges is caused by the decreased heat transfer from the plasma to the electrodes. No work has been found describing which is the predominant effect, especially at high energies.

Effects of short discharges

The fact that many of the experiments performed in this field exhibit different results depending of which parameter that is to be optimized, and under which conditions the experiments are performed, is exemplified by Maly and others who state that the optimum is a very short spark discharge (Refs 17,18,19,20,21). Experiments have been performed with discharges in the ns region showing positive results in terms of reduced emissions, fuel consumption and electrode erosion. This, as well as was the fact with long discharges, especially in lean mixtures.

The intentions of this thesis

The References 1-21 are all gathered from a review by Kalghatgi (29). Therefore, it is not known whether the above discussed results regarding long and short discharges are valid in a stagnant or turbulent environment. This thesis concerns the relation between flame propagation rate and dissipated energy, especially the energy in the breakdown phase, i.e. up to the first microsecond of the spark. These first parts of the energy are in the range 2 mJ to 120 mJ, thus far more than the minimum ignition energy. Therefore, it is likely that some of the results do not apply at this energy level. The experiments were performed in a static system, i.e. turbulence did not affect the results.

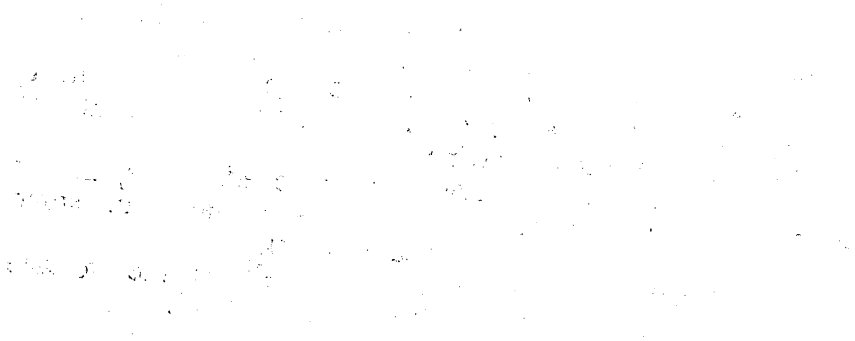

3. EXPERIMENTAL APPARATUS

The system consisted of a trigger unit, an ignition system, an oscilloscope, the high-pressure bomb and the gas handling system. All these parts are described below. They were connected as indicated in Fig.1 to enable the measurements.

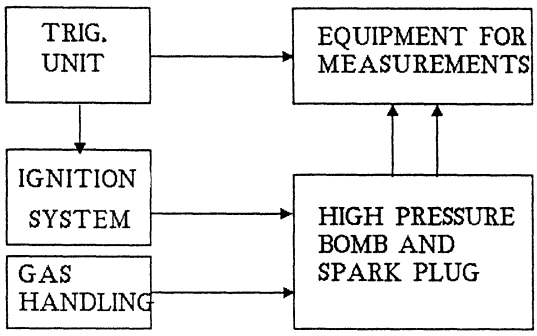

Fig.1: The set-up of the system

3.1 Discharge circuits

3.1.1 Capacitive discharge circuit

An ignition system based on a capacitive discharge circuit is now commercially available. Compared with an ordinary inductive system, it has some advantages:

-smaller spread in the time delay between the voltage pulse and the spark
-lengthens the lifetime of the spark plug
-better lean mixture operating conditions

The voltage across (Fig.2) and the current through the system can be divided into three parts:(values typical at 0.4 MPa)

-Before the breakdown, the voltage rises during typically 2 μs to the breakdown voltage, about 10 kV. Practically no current is flowing.
-When the breakdown voltage is reached, a spark is formed. Now a current arises, attains a value of some amperes, while the voltage decreases quickly.
-After the breakdown, the current as well as the voltage starts to oscillate and after some tenths of a millisecond equals zero.

One problem to be tackled was the fact that the discharge circuit was designed to work at a high repetition frequency and after an interval between two sparks longer than a few seconds, the spark showed characteristics quite different from the normal ones. In order to solve the problem, a second spark-plug, which gave a spark at a lower voltage, was connected to the first one. After a spark from this second spark-plug, it was quickly disconnected and another spark was generated, now from the first spark-plug.

3.1.2 Ultra-fast discharge circuit

In some regards the ultra-fast system exhibits completely different characteristics than the capacitive system:

-Breakdown voltage, about 20 kV, is reached after the order of 50 ns. (Fig.2)

-Coupled to the coaxial spark-plug the system has the capacity to deposit almost all its energy, of the order of 50 mJ, during the first 50 ns after the breakdown, the current attaining a maximum value of roughly 300 A.

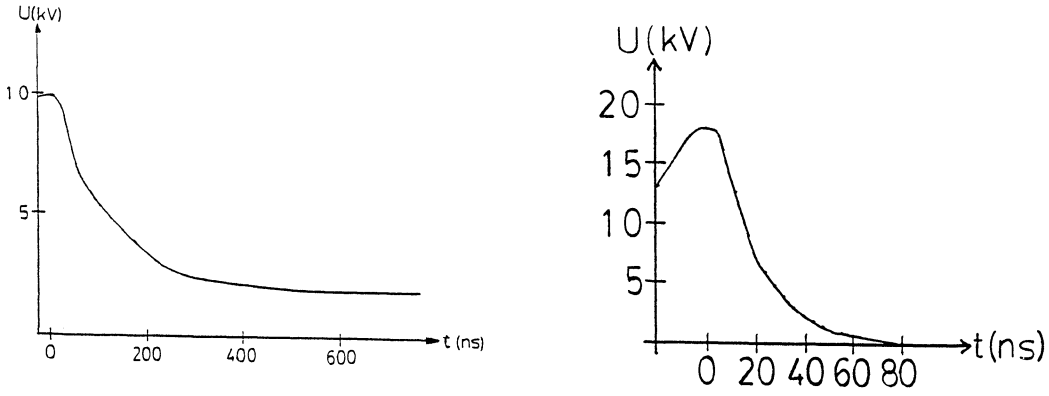

Capacitive Ultra-fast

Fig.2: The voltage of the capacitive and ultra-fast systems

The electrical arrangement can be seen in figure 3. When the thyratron is reached by a trigger pulse, the lower capacitor will be discharged through the thyratron, causing a voltage reversal on the lower capacitor. Both capacitors will now discharge through the 50-ohm transmission line, creating a voltage wave travelling through the coaxial cable. Voltage doubling occurs when the voltage wave arrives at the spark gap, until current begins to flow. Because of the long transmission line, reflected pulses will not appear more often than every 0.75 μs.(Ref.22)

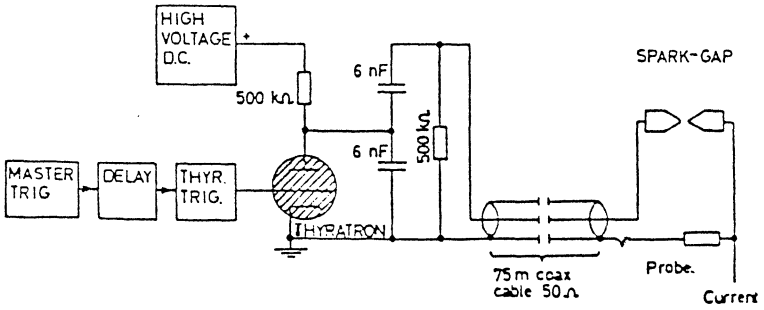

Fig.3: The ultra-fast discharge circuit

3.1.3 Spark plugs

In the second part of the experiment, where we examined whether the flame propagation speed was related to the energy dissipated, we used two different spark-plugs, one conventional one (NGK BCPR6ES) and one coaxial one (Fig.4). The coaxial spark plug consisted of two solid cylindrical bars, made of brass and 5 mm in diameter, threaded at their extremities. Two apices were mounted on the threaded ends. The apices were semi-spherical with a tip and made of stainless steel. This geometry gave very good reproducibility in the sparks, something that could never be achieved with the conventional spark-plug because of its rather large lower electrode. Both the spark-plugs were mounted in the middle of the high-pressure bomb.

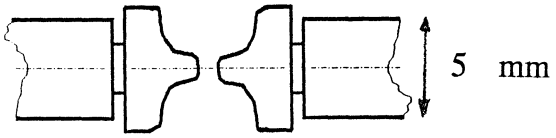

Fig.4: The coaxial spark-plug

3.2 The gas handling system

The centre of the gas handling system was the cylindrical, high-pressure reaction vessel. Its volume was 1 dm^3 with a inner diameter of 1 dm, and it had 2 inlets and 2 outlets. First the air was pumped out with a vacuum pump, then the premixed propane-air mixture was let in from the 10 dm^3 container in which it was mixed. The gas was ignited, and 10-20 ms after the spark a magnetic valve was opened to release the exhausts. To avoid the deposition of soot and condensed vapour, pressurized air was blown through the vessel before the next cycle (Fig.5).

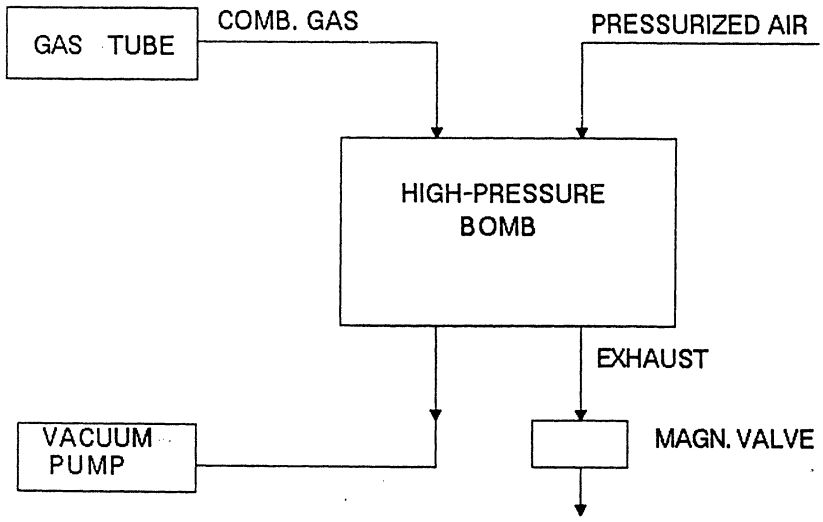

Fig.5: The gas handling system

The gas

The gas used was a mixture of 4.1 % propane in air, i.e. at stoichiometry. At these proportions, the flame propagation velocity varies relatively moderately with respect to changes in the proportions of propane and air. These proportions were chosen as the experiments were not performed with one unique filling of the gas container, but several different filling cycle where the proportions varied in the range 4.03 to 4.17 %. The pressure was 0.4 MPa.

The high-pressure bomb

The vessel was equipped with two windows, one on each side. Through these the spark plug could be inspected. The laser shadow-graphic system, discussed later, also made use of the two windows. The coaxial spark-plugs were inserted through the cylinder walls, diametrically opposite to each other, and were electrically isolated. Similarly, the ion probes were introduced as illustrated in Fig.9. The conventional spark-plug, on the other hand, was mounted on a bar, with its gap placed in the center of the vessel. The current going to ground potential did not return upwards through the spark-plug, but continued through a pin welded onto the outer electrode to ground along the same axis as the bar and the spark-plug.

3.3 Electrical measurements

3.3.1 Measuring the voltage of the spark

It can be quite difficult to measure the voltage of spark due to the strong elctromagnetic fields emitted from the spark and the ignition system. In the case of the capacitive system, a high voltage probe with an attenuation of 1000 times was connected directly to the spark-plug. The signal was then analysed on an oscilloscope, and the noise level was found to be low. In the case of the ultra-fast system however, the noise levels with this coupling were intolerable.

Optical measurement of high voltage

Supression of the noise was possible by transforming the electrical signal into an optical signal by means of a capacitively coupled Pockels cell, as proposed by Hertz (Ref.22). This method was also used succesfully in earlier projects (Ref.26). It consists of a Pockels cell, a crystal which changes the polarization of the incoming light proportionally to the high voltage imposed, capacitively coupled via an antenna to the spark-plug. The voltage of the spark-plug is divided between the capacitance in the air between the spark plug and the antenna, and the capacitance of the crystal (Fig.6a). By changing the position of the antenna, the capacitance in the air changes and hence the voltage over the Pockels cell. This is important due to the lack of linearity when applying too high voltages over the crystal.

A polarized laser beam is transferred through the Pockels cell and the change in polarization is analysed by a second polarizer after passing through the crystal. The change in intensity of the laser beam is proportional to the voltage of the spark-plug within a linear range (Fig.6b). The laser beam was focused onto a biased photo-diode 30 m from the spark, and the signal from the diode was registered by photographing an oscilloscope screen. The photographs were then measured at every 4 ns, or if adequate 8 ns. Attempts were made to use a transient digitizer, but its sampling rate of 100 MHz proved insufficient. Before measuring, a careful calibration had to be performed. The pressure in the bomb was increased so that no breakdown occurred. Then no noise disturbed the measurements, and the voltage probe and the Pockels device could be used simultaneously. Some well defined values of voltage were applied to the spark-plug, and the corresponding signals from the diode were plotted versus the voltage, thus generating a calibration coefficient in the linear region.

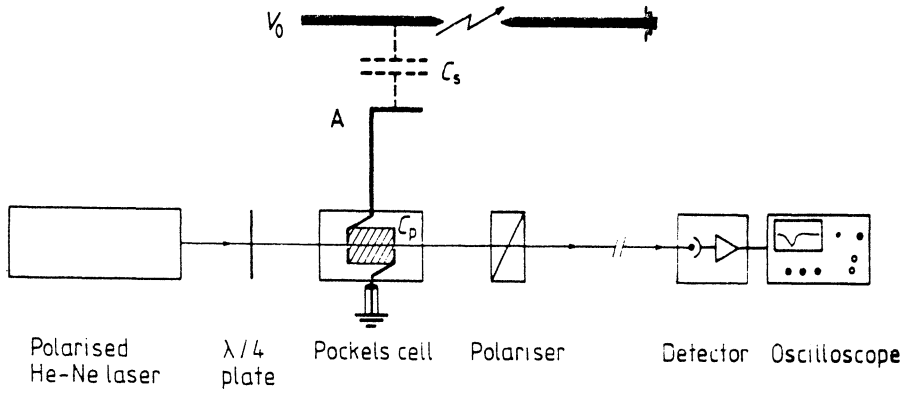

Fig. 6a: The Pockels cell device. The antenna A connects the Pockels cell electrode and the HV electrode via the capacitance C_s.

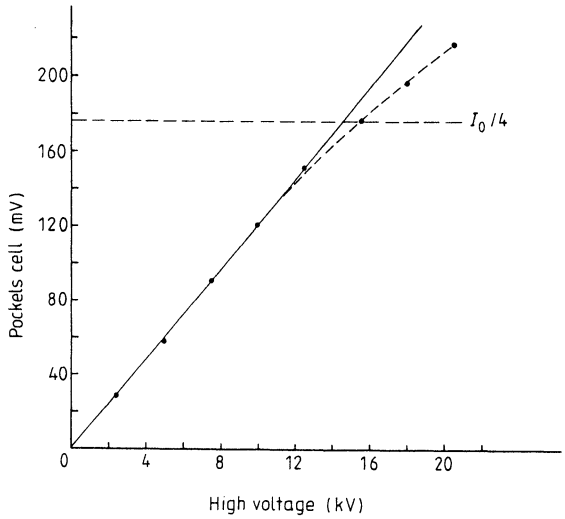

Fig.6b: Test of linearity of the Pockel's cell device. "Pockels cell" denotes the voltage of the detector.

3.3.2 The current probe

The spark current was measured by a specially designed current probe, which was mounted on the combustion chamber. It consisted of two basic parts, a resistor made from a thin canthal foil and a coaxial envelope. When a spark is formed, the current is flowing radially through the circular foil, hence no undesired inductances are formed. The current is detected as a voltage over the foil and is monitored on a fast-storage oscilloscope. Also see Fig.7.

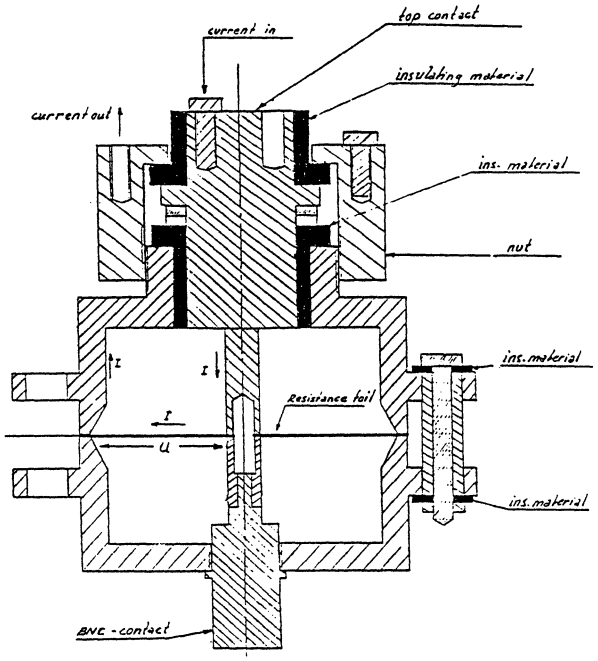

Fig.7: The current probe

4. DETECTING THE FLAME FRONT

4.1 The flame-front

The flame consists of several different zones. The leading zone is a region where the gas is heated up before reacting. The typical temperature here is 400°C. Following this comes the reaction zone where the reaction takes place. Here the temperature is 1000-2500°C, and the concentrations of ions, light-emitting molecules and radicals are high. The flame is only a few tenths of a mm thick, and the separation between the heating zone and the reaction zone is only around a tenth of a mm. Detection of the flame front can be performed in several ways. In this project three methods were used concentrating on different features of the flame. Laser shadow-graphics detects the variation in the refractive index, which is most predominant around 400°C, i.e. the first zone. Both ion concentrations and light emitting particles are, on the other hand, the most marked in the warmer second zone. This causes a slight difference in the detection, since the laser system detects the first zone, and the other two the second zone. However, the difference is less than the resolution limits.

4.2 The laser shadow-graphic system, our reference

The system used as a reference system in the detection of the flame position is the laser shadow-graphic system. A similar set-up has been used with reliable results in previous projects (Ref.26). It is based on the fact that the warm burning gas in the flame has a different refractive index from that of the unburnt gas surrounding it. A beam from a Nd-YAG laser is expanded to a diameter of 5 cm. Coming from the side window of the bomb, the beam passes the flame and is refracted there as if it were a negative lens. The shadow of this "lens" is then projected through the other window onto a film. This film is analysed in an Abbe comparator, a device based on a microscope with a resolution of 10 microns. See Fig.9.

A resolution of 300 microns

The resolution of this method is not limited by the comparator, but by the fringe pattern that arises due to diffraction of the laser beam. Since the distance to a specific fringe was measured the accuracy was around 200 microns. The laser pulse itself had a duration of 0.1 ms which also blurs the shadow by some 200 microns. The total resolution was thus around 300 microns.

4.3 The fibre-optic system

In one of the detection systems a fibre-optic pick-up was used. A fibre-tip was mounted on a track in the spark plug using two-component epoxy resin, and the fibre was connected to a photo-multiplier, which was connected in turn to an oscilloscope (Fig.8a). The fibre-tip was situated 5.5 mm from the spark-plug centre, viewing parallel to the plug axis. When the flame front propagates underneath the pick-up, its light is transferred into the fibre, and a signal originating from the propagation of the flame is detected. Several fibres can be used in order to overcome the problem of the asymmetrical propagation of the flame.

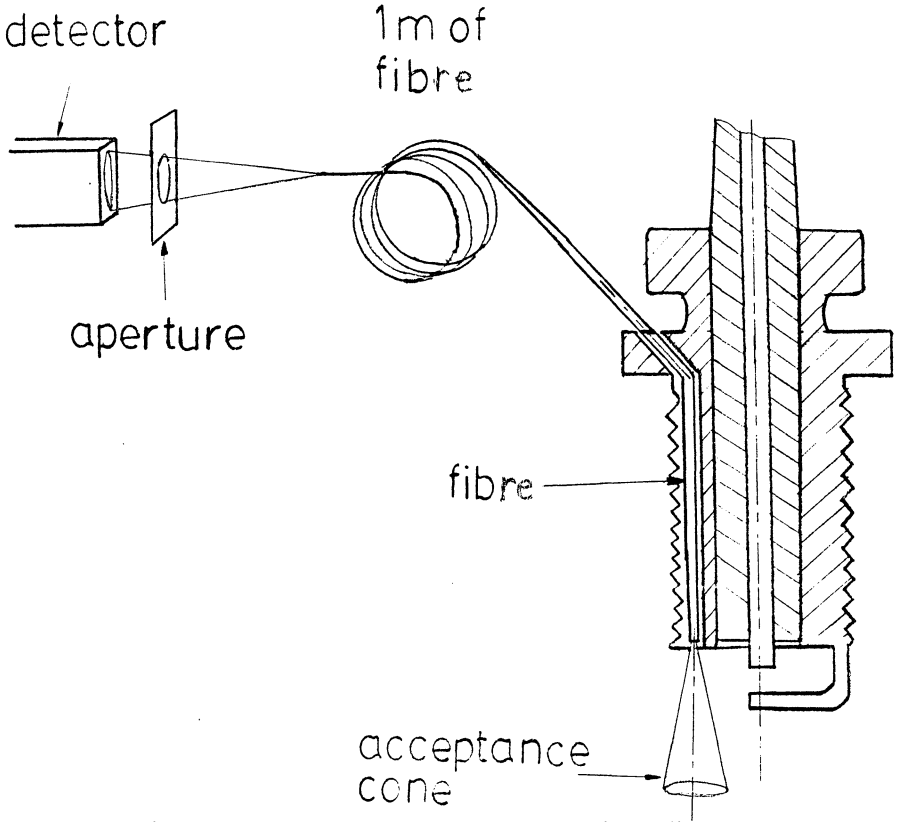

Fig.8a: The mounting of the optical fibre

Controlling the risetime and light intensity

Geometrically, the fibre has an acceptance cone within which light is permitted to pass into the fibre, while no light from outside this cone is transmitted into the fibre. The flame front propagates almost spherically towards the cone, and when the two intersect, light from the front starts to pass into the fibre. As the front moves into the cone, the signal rises to a maximum value and, after a slight overshoot, is more or less constant (Fig.8b). The rise time of the signal is dependent on the top angle of the cone. The narrower the cone, the shorter the rise time. The disadvantage of a narrow cone is that less light is collected, thus making the detection more difficult. In our case, the prime problem was shortening the rise time, as the light had sufficient intensity, and effort was put into narrowing the angle.

Narrowing the angle of acceptance

The angle defined by the fibre itself was theoretically 35 degrees, but as only 1 metre of fibre was used the reflections in the cladding were not attenuated, and thus the angle increased. Other fibres, e.g. monomode-fibres, have a very narrow angle but the area of the core is hundreds of times smaller than the one we used, and consequently the intensity of the light is reduced accordingly. In order to decrease the angle, the tip of the fibre was burnt in a flame so that it melted slightly and reshaped into a lens. The resulting fibre had an angle of acceptance of 25 degrees, which proved sufficiently narrow. This method of lens-tipped fibres has a disadvantage since it is difficult to produce fibre tips with a well defined angle of acceptance. A method was proposed by Russo et al. (Ref.23), using energetic laser pulses. It is likely that methods other than lens-tipping may be superior in narrowing the angle.

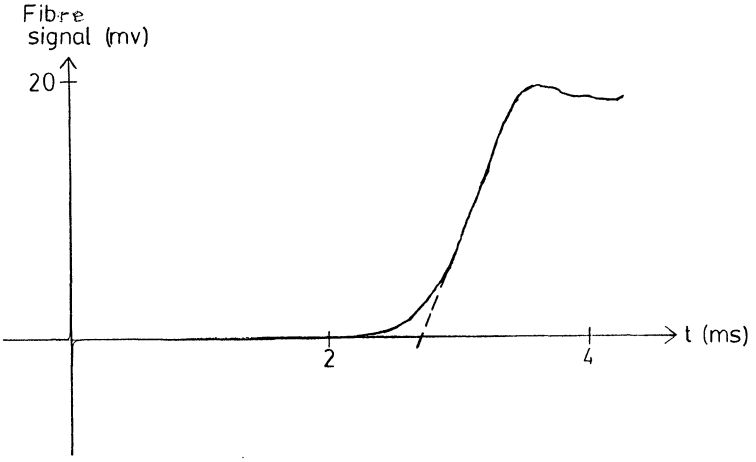

Fig.8b: A typical signal from the optical pick-up

Narrowing by means of apertures

Another method of narrowing the angle is to use an aperture. If the fibre tip is placed in the track in the thread, the track itself acts as an aperture. This would also protect the fibre from the intense heat inside the cylinder. An aperture can also be introduced after the fibre, before the detector (Fig.8a). Provided that the fibre is only about 1 m long, the angle of incidence for a specific ray is maintained through the fibre and equals the angle when exitting the fibre. This means that if large-angle rays are blocked after the fibre by means of an aperture, these are the same as would have been blocked if the aperture had been placed before the fibre i.e. inside the cylinder. This latter method has the advantage that the aperture can be changed when necessary if it is found that the intensity of the light is too low or the rise time is too long, which is not possible if the fibre is placed in the track and glued in.

The lifetime the fibre is several hours

The lifetime of this arrangement is limited mainly by soot deposition on the fibre tips, but Spicher and Kollmeier (Ref.24) have reported that the results are not affected by this deposition for several hours of operation. Personal contacts with Sandia laboratories revealed that they too have had an operating system in use for several hours, which terminated when the fibre fixture mechanically cracked the fibre.

Photo-multiplier not necessary

The detector used was a photo-multiplier, but the high voltage was only 500 V of a maximum 1300 V allowed, so undoubtedly a photo-diode or photo-transistor would be sufficient, if the whole spectrum is used. Because the rise times are around 0.5 ms, there is no need for a fast diode or transistor. The fibre should have a core diameter of 150-300 microns to gather enough light, and the material in the cladding should be the same as in the core, i.e. quartz/quartz or glass/glass. This is in order to avoid cracking due to different thermal expansion rates in quartz and glass.

Agreement between methods with less than 6% error

The correlation between the results obtained with the fibre-optic pick-up and the flame propagation was measured with the laser shadow-graphic system as a reference. A major problem in this measurement is the fact that the laser method tells us where the flame is at a certain time, whereas the fibre-optic pickup tells us at what time the flame is at a certain spot. One method could have been to let the fibre-optic signal trigger the laser, but the laser has a 0.2 ms delay which made this impossible. Instead, we shot 22 shots with the laser delayed between 1.6 ms and 2.6 ms, with the corresponding fibre-optic signal recorded for each shot. The position of the flame was measured on the film in an Abbe comparator, and a mean velocity of 3.3 m/s was calculated from these positions. In order to reconstruct where the flame was at the time of the fibre-optic signal the difference in time between the laser pulse and its corresponding signal was multiplied by the mean velocity, thus producing an estimated distance of travel during this time. This distance is then added to the known position, i.e. at the time of the laser pulse. This sum is the estimated position of the flame at the time of the fibre-optic signal. Had this system been perfect all these positions would have equalled the position of the fibre-tip, The result is that the mean position is 5.6 mm and the standard deviation is 0.34 mm i.e. 6%. The disadvantage of this method is the assumption of a constant and shot-to-shot stable velocity. The influence of this error decreases the closer the flame gets to the position of the pick-up, therefore, some of the shots, where the flame by the time of the laser-pulse is far from the pick-up, are rejected. Still this erroneous assumption affects the result and the true correlation is believed to have an error no greater than 6%.

Possible future developments

The light coming from the fibre can be used for other purposes than simply detecting the propagation of the flame. If it is spectrally analysed, peaks originating from different radicals can be identified, and for example, the temperature of the flame can be derived from this. Possibly compounds prominent in forming the exhaust can also be quantified, which is of great importance in minimizing these. This, of course, demands more sophisticated equipment than was used in our experiments. It may also be possible to detect knocking, which would add as a higher frequency signal to the original step-like signal. Since the experiments were not performed under knocking conditions there are no experimental data to support this hypothesis. A knock sensor based on optical pick-ups has now been presented by Sandia Laboratories, and is commercially available (Fig.20, p.35).

4.4 Ionization probes

The principle

A technique which uses the previously mentioned fact, that the flame front is partially composed of ions, is used in ionization probes. The ionization probe consists of a small-diameter conductor which is electrically insulated from its surroundings. The probe is mounted in the combustion chamber, with its tip at a fixed distance from the spark centre. As the electrically conductive flame front passes the probe, some of the ions will adhere to the probe, and a difference in voltage will arise between the probe and the combustion chamber wall. This difference in voltage is detected and indicates the arrival time of the flame front at the probe.

The experimental arrangement

Since two different spark-plugs were used during the experiments, two different ion probes had to be designed. When the coaxial spark-plug was acting as ignition source, a probe made of a stainless-steel-tipped copper wire, 2 mm in diameter, was used. The probe was led through the chamber wall and its tip was located on the surface of a sphere, with a radius of 4.5 mm and its centre midpoint between the electrodes (Fig.9).

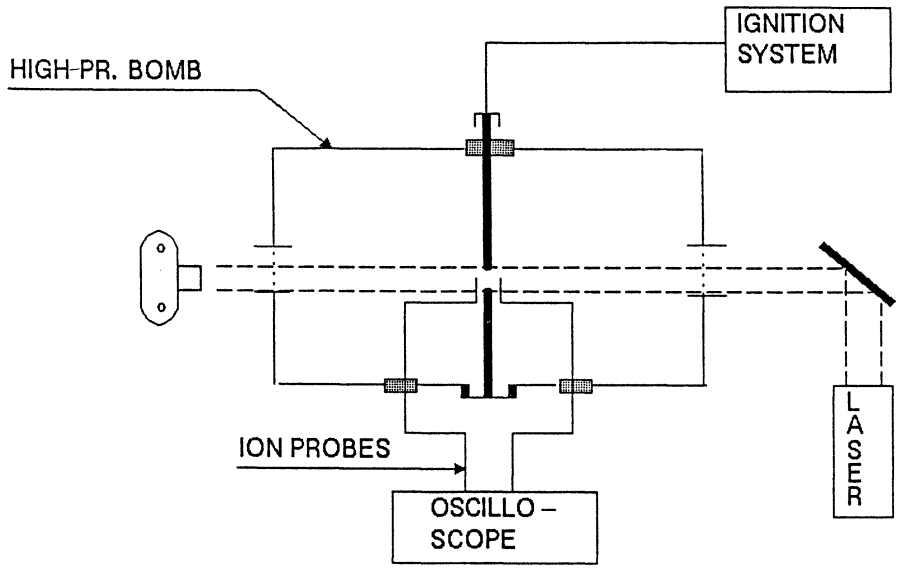

Fig.9: Set-up for the ionization probes, and the laser shadow-graphic system

The other arrangement demanded a thinner probe, since it was glued in a track along the conventional spark-plug. A 0.7 mm copper wire was chosen. The probe tip protruded approximately 2 mm from the body of the spark-plug, and was placed on the surface of the same sphere mentioned above.

The behaviour of the signal

The signal, detected on an oscilloscope, is very similar to the one received from the fibre-optic system, but the rise time is longer, about 1 ms. It is important to reduce this time to a minimum. To achieve this, the ion probe was positioned in several different directions, and signals were recorded from each one. (See "Ion probe positioning") The result of these experiments was that if the probe was parallel to the axis of the spark-plug and the tip was on a level with the centre of the electrodes, a minimum was reached. One reason for minimizing the rise time is that the experiments showed that there is a possibility of detecting knocking through a high-frequency signal superimposed on the original signal. With both types of probe a sharpening of the probe tip slightly diminished the rise time. Generally the copper probe tended to give more reproducible signals than the steel-tipped probe, which sometimes exhibited immense pulses in the middle of the "normal" signal.

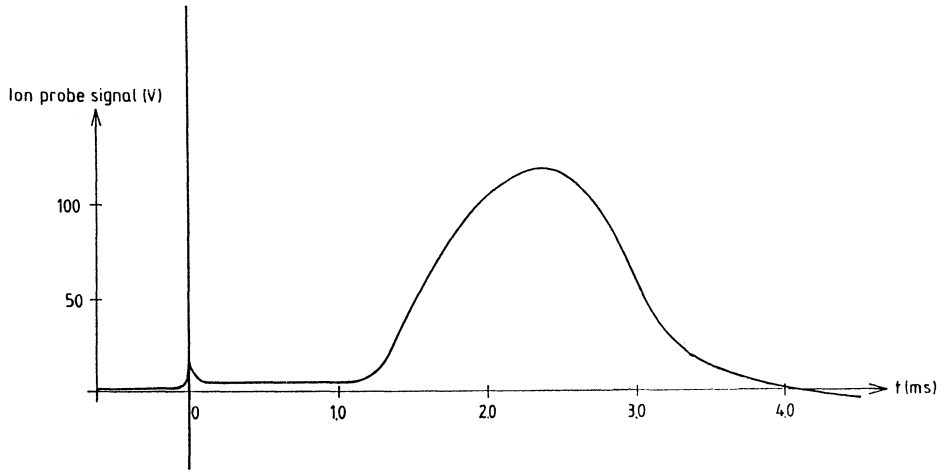

Fig.10: The copper probe signal

Correlation

The procedure of determining the accuracy of the ion probe, essentially follows the description of correlation between the fibre-optic pick-up and the flame propagation, with one exception; special consideration had to be given to photographs where the flame front had passed by the ion probe, since the latter may disturb the former. The calculation resulted in a mean position of 4.4 mm and a standard deviation of 0.46 mm i.e. 10 %. As mentioned before this method assumes a constant flame front velocity, which is doubtful. Hence the relatively large standard deviation, which is also caused by few adequate data. When performing the correlation experiment, two ion probes were used, symmetrically surrounding the spark-plug.

Other applications

It is also of great interest to measure the temperature of the passing flame front. In this field the ionization probe technique provides us with an instrument (Ref.25), although it seems necessary to make use of a double-probe technique, similar to the single-probe technique used in this work. A double-probe consists of two probes situated in the combustion chamber. A variable voltage source is connected between them and the current, which rises as the flame front passes by, and is measured in an external circuit. The temperature is determined from the size of the current. In consequence leakage currents must be controlled.

Ion probe positioning

In order to achieve an optimal signal with regard to the rise time and the reproducibility, an experiment with double ionization probes (see "Other applications") was performed. The double probe was mounted in the combustion chamber at a fixed distance from the coaxial spark-plug, which was connected to the ultra-fast discharge circuit. Six signals were recorded originating from different probe geometries. The resulting signals can be seen in Fig.18 in the appendix. Two conclusions can be drawn. The shortest rise time appears when the probe is parallel to the spark-plug, with its tip on a level with the centre of the spark-plug electrodes. When the two probes, which make up the double probe, form an angle of approximately 75 degrees to each other, it seems that the rise time is even shorter than when they are parallel to each other, but the reproducibility is poorer in the former case. Furthermore, the experiment revealed the superiority of the single probe over the double probe as far as reproducibility is concerned.

5 RESULTS OF THE MEASUREMENTS

5.1 Evaluating the energy

In this experiment, we have tried to establish a connection between the flame front propagation rate and the energy dissipated in the spark. The propagation rate was determined by means of a technique utilizing ionization probes and the energy was calculated as the integral over the measured quantities voltage and current. The voltage was monitored on an analogue oscilloscope and then photographed with an ordinary oscilloscope camera, while the current was recorded digitally on a storage oscilloscope. The curves were then divided into small sections which were treated as being linear, a procedure which facilitates the calculation of the integral. Under constant conditions (spark-plug, spark gap, pressure and ignition circuit), the current appeared to a great extent to be similar from spark to spark, which was not the case with the voltage. Accordingly, different values of the energy were calculated from different voltage curves matching only one current curve. Two parts of the energy were identified, the first part of the energy, 0-1 μs, and the total energy.

5.2 The performance of the capacitive system

In the experiments both a conventional spark-plug and a coaxial spark-plug were used with the capacitive ignition system. The difference in behaviour is both temporal and in the magnitude of the power. With the conventional spark-plug the system has a maximum power of around 11 kW after 30 ns, and the first part of the energy is deposited after 500-600 ns (Fig.11 and Table 4), whereas the coaxial spark-plug has a maximum power of 220 kW after 10 ns, and the first part of the energy is deposited after 50 ns (Fig.12 and Tables 5,6). However, the first parts of the energy are not as different as the powers, which are 1.4 mJ with the conventional, and 3.7 mJ with the coaxial spark-plug. The total energy is about the same, 10 mJ with the coaxial and 17 mJ with the conventional spark-plug.

Rapid current oscillations

In the case of the coaxial spark-plug an interesting behaviour arose as the spark gap was altered from 0.8 mm, which was the gap of the conventional spark-plug, to 1.05 mm, which was the gap when using the ultra-fast ignition system. Instead of the normal current, a fast rise and a smooth decrease back to zero, a 60 MHz attenuated oscillating current appeared (Fig.12). Reactive power, which is the result of this, drains the spark of energy. The oscillation is the result of a change in the inductance, the capacitance and the resistance of the spark and spark-plugs. The circuit is very sensitive to these variations, and the current and voltage differ significantly with small changes. It is possible to avoid these oscillations by adjusting the parameters mentioned above. (Calculations like these are performed by Prof. T Högberg of the Lund Institute of Science & Technology.)

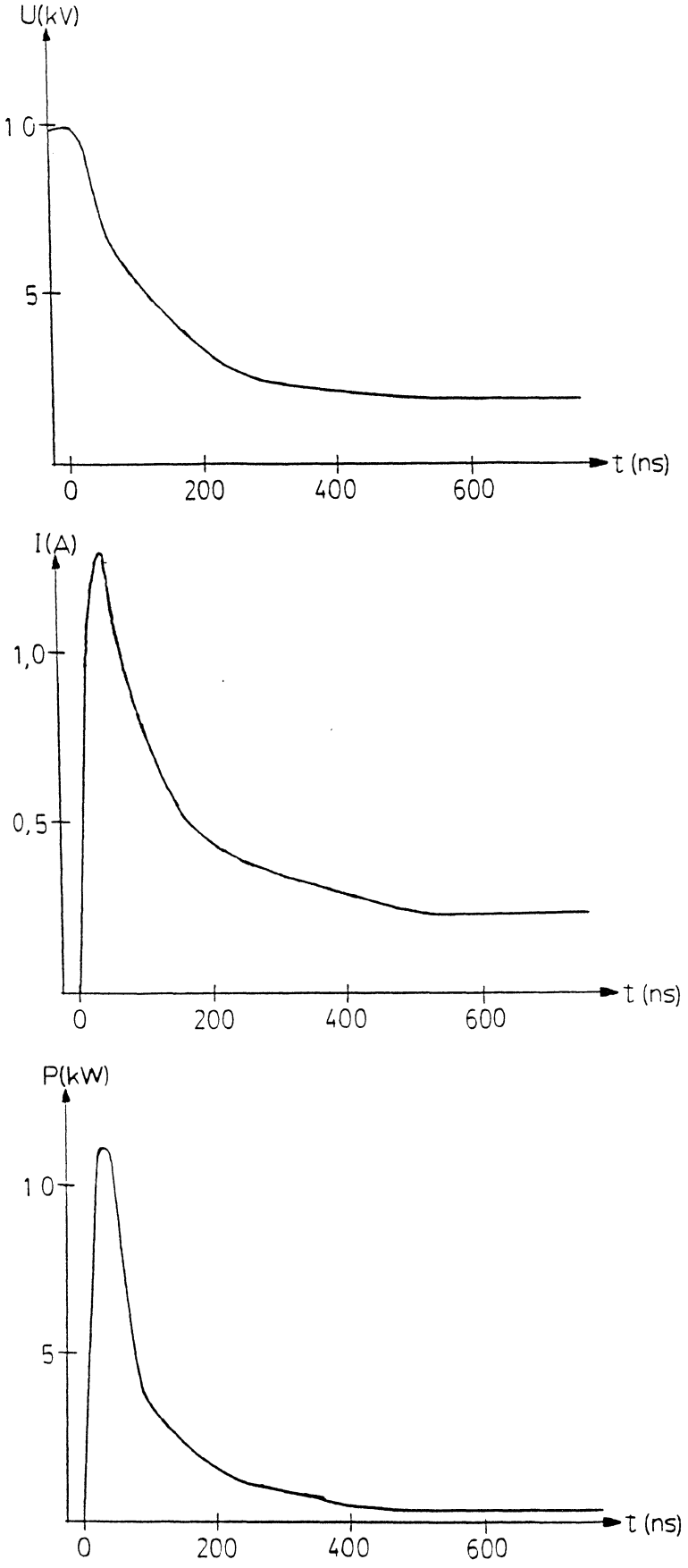

Conventional spark-plug

Fig.11 Temporal behaviour of the capacitive system. Shot-to-shot variations of the current were much larger with the coaxial spark-plug (0.8 mm gap) than with the conventional one. The oscillating current of the 1.05 mm gap spark-plug was almost identical for different shots.

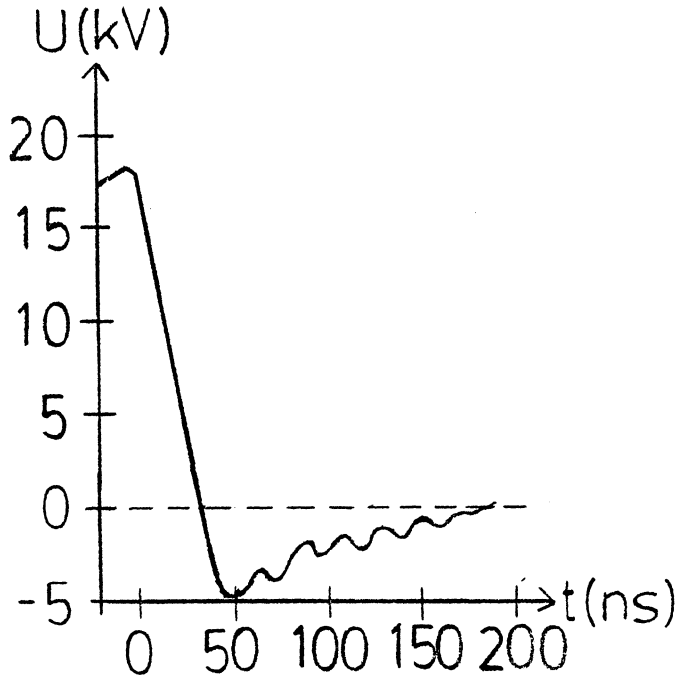

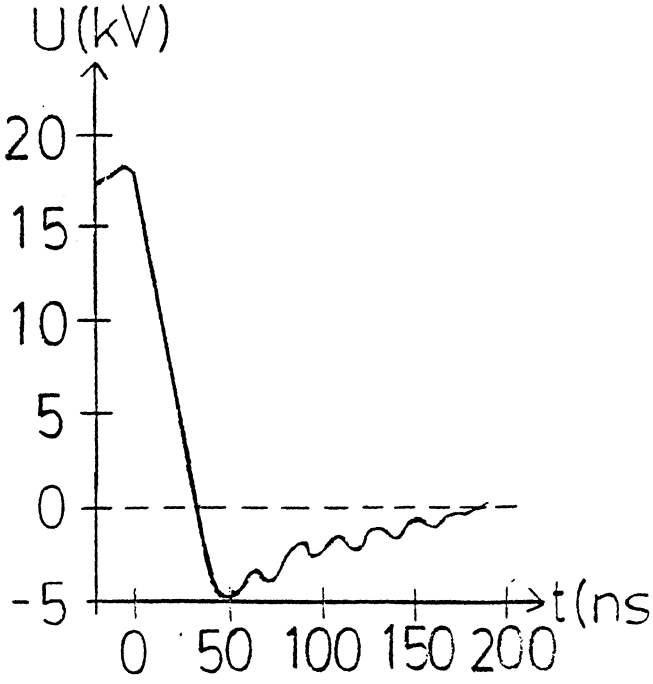

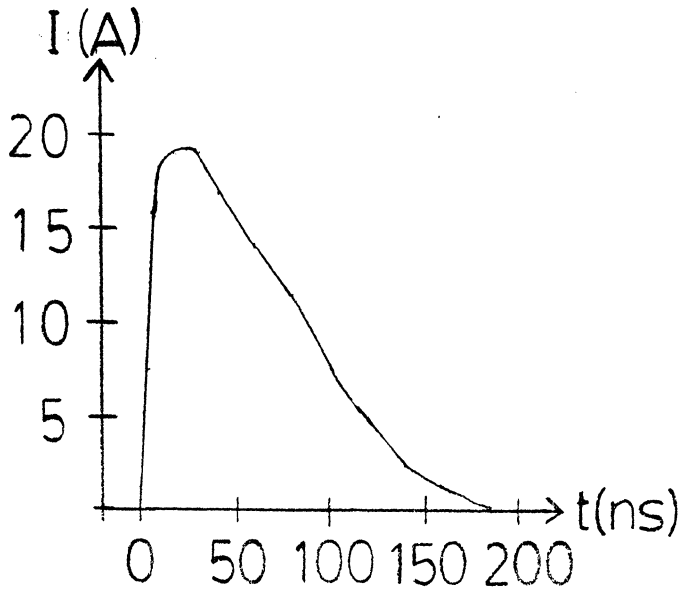

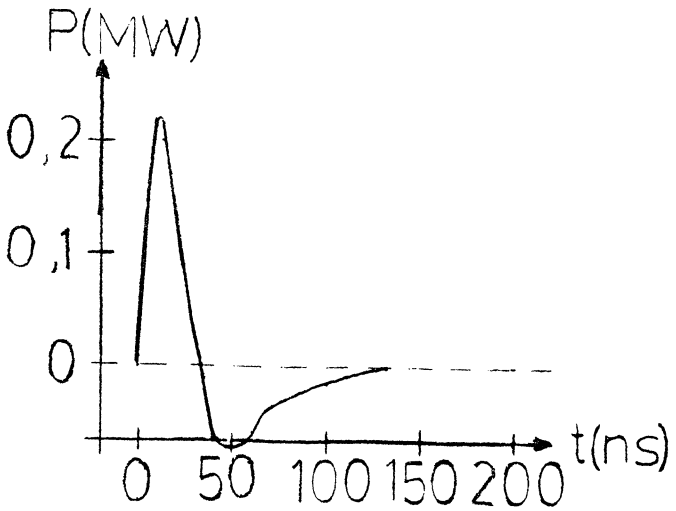

Coaxial spark–plug,
0.8 mm spark gap

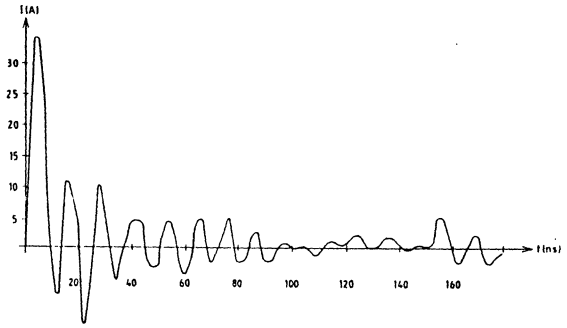

Coaxial spark–plug,
1.05 mm spark gap

Fig.12 Temporal behaviour of the capacitive system.

5.3 The performance of the ultra-fast system

The same spark-plugs were used with the ultra-fast system as with the capacitive system. When using the coaxial spark-plug the total energy was deposited within less than 100 ns. Then, of course, the first part of the energy equals the total energy. The energy of the spark can be varied by varying both the capacitors of the discharge circuit and by altering the high voltage over the thyratron (see "Ultra-fast discharge circuit", p.6). Typical values of the energy were 50-100 mJ (See also tables 1,2,3).

The current and the voltage behave differently when the conventional spark-plug is connected. The voltage after the breakdown decreases 10 times slower and does not equal zero until some hundred μs after the breakdown. The maximum value of the current is diminished 40 times and it exhibits the same type of oscillations as discussed above, though at a different frequency, 6 MHz (Fig.13).

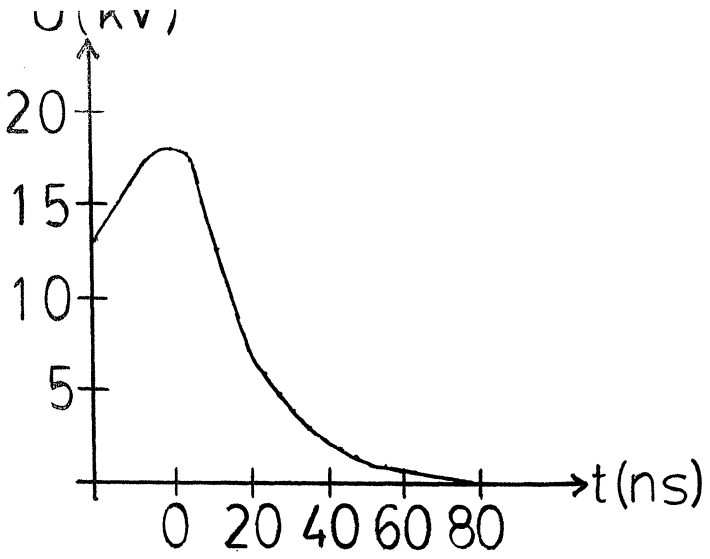

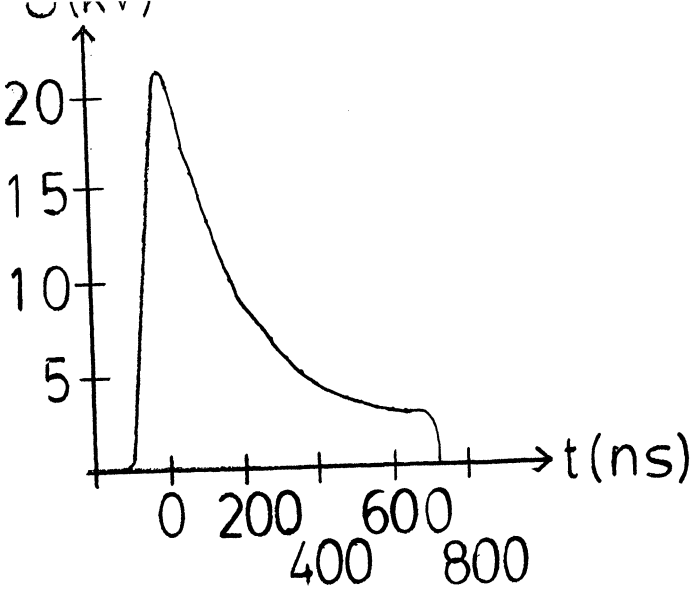

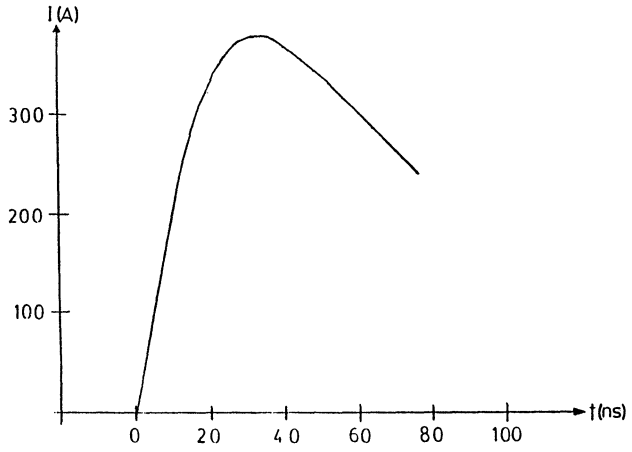

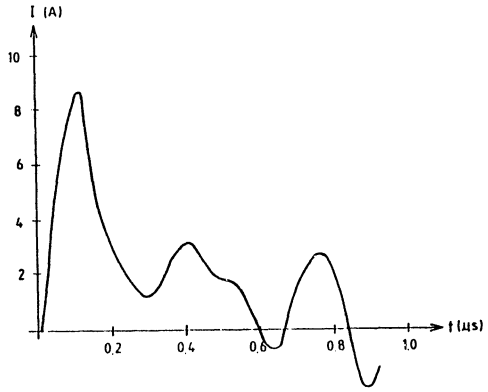

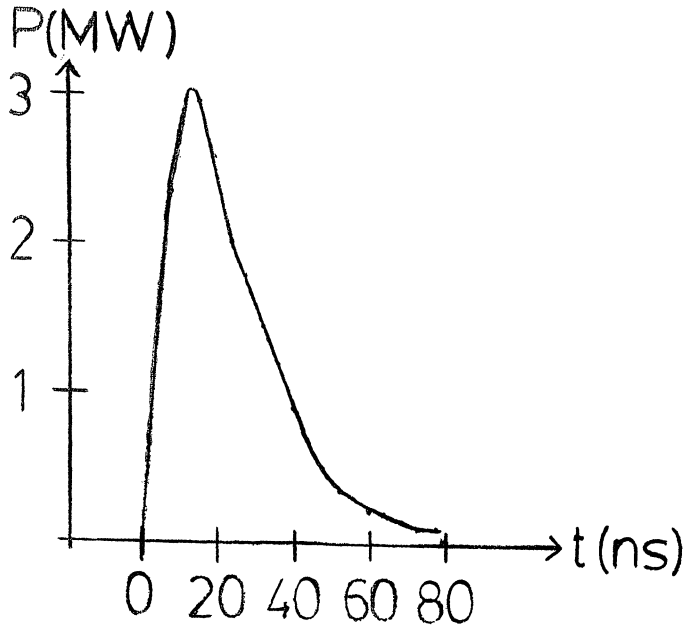

Coaxial spark plug

Conventional spark plug

Fig.13 Temporal behaviour of the ultra-fast system.

5.4 Flame front velocity measurements

The time required by the flame to reach the ionization probes 4.5 mm from thespark-plug was also measured. From this was the mean propagation rate of the individual shots calculated as 4.5 mm divided by the measured time expressed in ms. These experiments were performed partly to investigate the coupling between energy and propagation rate, hence the big difference in energy between the sparks. Especially interesting was the relation between the energy dissipated during the first microsecond after the breakdown and the propagation rate. The resulting data are presented in tables 1-6 and are discussed in the next chapter (in Figs 14-17). The data are presented in diagrams. When performing the experiments two different spark-plugs were used to aquire a large variation in the energy. The geometry may affect the propagation rate, and therefore the diagrams are separated with respect to geometry.

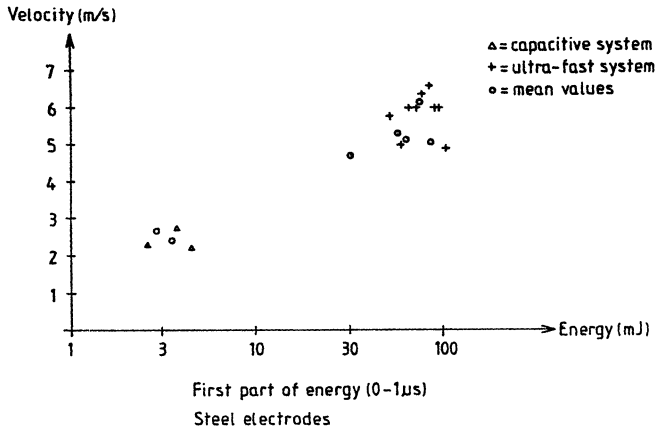

Fig.14: Results from experiments with the coaxial spark-plug. Crosses and triangles are individual shots with corresponding velocities and energies. The circles are values originating from a different procedure: the energy from one shot was calculated. Then several shots were performed where the propagation rate was measured and a mean value was calculated. This mean value was plotted versus the energy from the single shot.

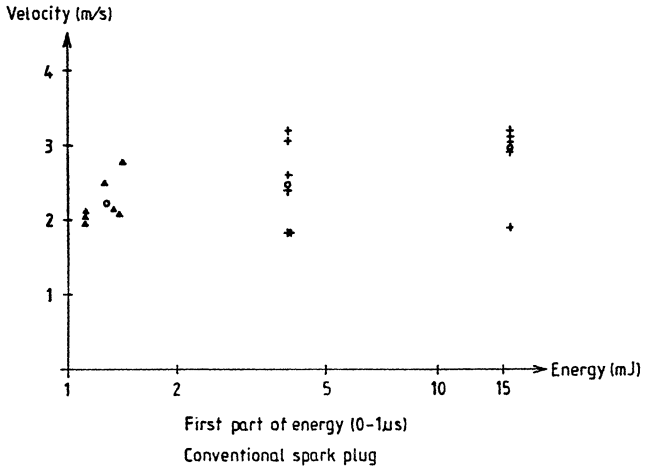

Fig.15: The results from the conventional spark-plug. The reason why the energies of the ultra-fast system all equal two values is that the voltage curves were almost identical, and thus only two curves were used in the calculation.

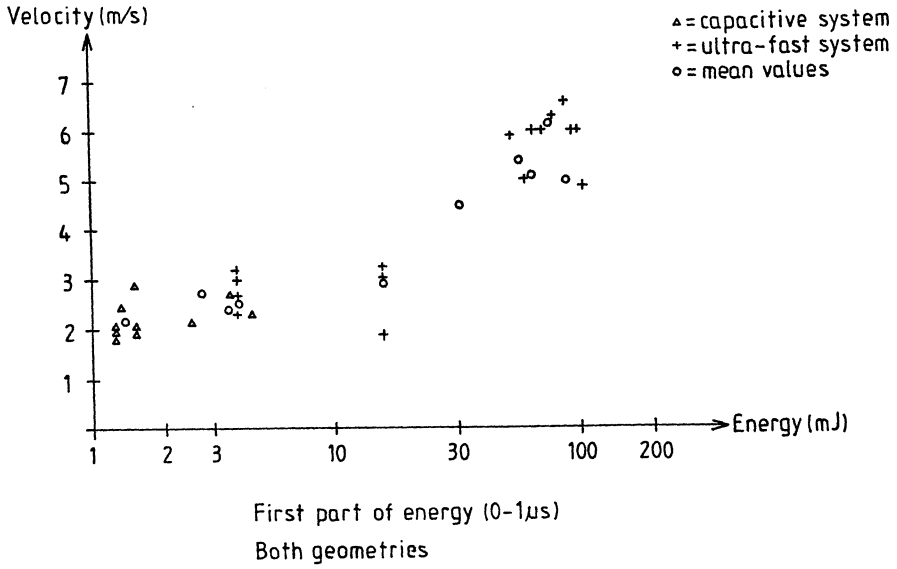

Fig.16: In this diagram, the data from fig.14 and fig.15 are plotted together.

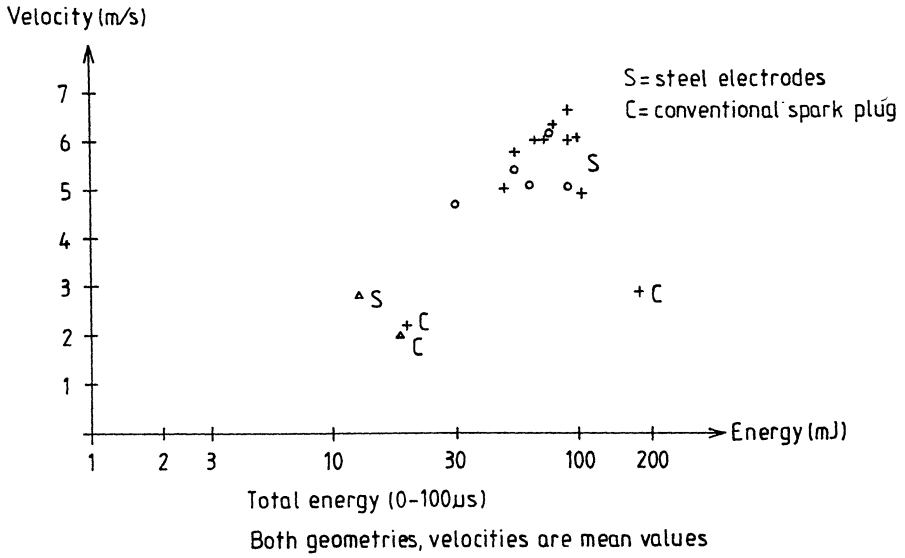

Fig.17: The velocities were measured at different shots than the energy. Thus the velocity associated with an energy is the mean of several shots. These were performed at equal conditions as when measuring the energy. The notations S and C indicate the different spark plugs, where S stands for the coaxial spark plug. In the upper right corner S denotes the entire cluster of data.

6 CONCLUSIONS AND DISCUSSION

Geometrical effects

In previous projects (Ref.26) it has been found that the minimum energy required for ignition depends on the geometry of the spark-plug. This is partly the result of fractions of the energy being lost in heating the electrodes. Larger electrodes increase the minimum energy (Ref.27). Despite the difference in size of the two spark-plugs used in our experiments, the effect of the geometry was not noticeable, possibly due to the fact that the experiments were not performed to investigate the minimum energy, thus the lack of adequate data makes it difficult to draw any conclusions.

Energy - Propagation rate

The experimental results demonstrate a coupling between the flame propagation rate and the energy deposited, particularly the first part of the energy (0-1 μs). As seen in Fig.16 the propagation rate is relatively constant as a function of the first part of the energy up to values of 15 mJ. Beyond this energy, the propagation rate increases with increasing energy, at least up to 100 mJ.

First part of the energy the most important

Similarly, in Fig.17, there is a dependence between the total energy and the propagation rate after 15 mJ, with the important exception of the largest energy of 186 mJ only having a corresponding propagation rate of 2.8 m/s. This particular measurement exhibited a relatively small first part of the energy (16 mJ), compared with the total energy. The first part of the energy appears to be a more important parameter than the total energy in determining the flame propagation rate.

Possible explanations

There are two main explanations of the dependence. Firstly, the first part of the energy determines the temperature of the plasma, which in turn determines the concentration of radicals in the ignition process. An increase in this concentration accelerates the propagation rate chemically.

Secondly, a large, hot plasma produces a shock wave, a pressure wave that propagates faster than the speed of sound, and is attenuated inversely proportionally to the distance from the spark. The gas is heated as the shock wave passes, and this heating increases the propagation rate of the flame front (Ref.28).

Static or dynamic system

The measurements were carried out in a static system, which eliminates the effects of turbulent gas flow. The minimum energy required for ignition and the optimum spark duration are affected by the flow velocity (Ref.27). It is likely that the coupling between the energy and the propagation rate is also influenced by this flow velocity. Further investigations should be performed in a dynamic system, either at a nozzle where the flow velocity is well defined, or in an engine where it is turbulent.

Current oscillations

A model for the rapid current oscillations has been developed by Prof. T. Högberg at Lund Institute of Science &Technology. It is possible to avoid these undesired oscillations by matching the attenuation coefficient to the applied voltage pulse in the ignition circuit. This voltage should be much larger than the breakdown voltage.
(The attenuation coefficient is dependent on the inductance, the capacitance and the non-linear resistance function of the spark gap.)

Detection systems

During this project two systems for detecting the flame front at a given distance were investigated and developed, one using optical fibres and the other using ionization probes. Both can be used in dynamic systems, such as inside the cylinder of an I.C. engine, and provide real-time data. Recently an optical probe has become commercially available, which can be used as a knock sensor, similar to our system. Further investigation of the shock wave demands a high-speed camera (10 kHz), or a pulsed laser with a high repetition frequency, e.g. a Cu-vapour laser or possibly a solid state laser.

7 REFERENCES

(1) Soltau, J.P., Proc. Inst. Mech. E.,2, p.99, 1960-61

(2) Peters, P.D., and Borman, G.L., SAE Paper No. 700064, 1970

(3) Arrigioni, V., Calvi, F., Cornetti, G.M. and Pozzi, U., SAE Paper No. 730088, 1973

(4) Winsor, R.E. and Patterson, D.J., SAE Paper No. 730086, 1973

(5) Barton, R.K., Lestz, S.S. and Meyer, W.E., SAE Paper No 710163, 1971

(6) Tromans, P.S., Fluid Mechanics of Combustion systems, (Ed.s Morel, T., Lohman, R.P. and Rackley, J.M.) p.201, ASME publications, 1982

(7) Kalghatgi, G.T., Combust. Flame, 60, p.299, 1985

(8) Dale, J.D. and Oppenheim, A.K., SAE Paper No. 810146, 1981

(9) Rose, H.E. and Priede, T., Seventh Symposium (International) on Combustion, p.454, Butterworth, London, 1959

(10) Rose, H.E. and Priede, T., Seventh Symposium (International) on Combustion, p.436, Butterworth, London, 1959

(11) Kono, M., Kumagai, S. and Sakai, T., Sixteenth Symposium (International) on Combustion, p.757, The Combustion Institute, 1977

(12) Desoete, G.G., International Conference on Combustion in Engineering, Vol.1, p.93, I. Mech E., 1983

(13) Aiman, W.R., Combust. Sci. Tech., 15, p.129, 1977

(14) Nakai, M., Nakagawa, Y., Hamai, K and Sone, M., SAE Paper No. 850075, 1985

(15) Hancock, M.S., Buckingham, D.J. and Belmont, M.R., SAE Paper No. 860321, 1986

(16) Yamaguchi, J., Automotive Engineering, Vol.92, No.11, p.89, Nov. 1984

(17) Maly, R. and Vogel, M., Seventeenth Symposium (International) on Combustion, p.821, Combustion Institute, 1979

(18) Maly, R.R., "Spark ignition: Its physics and effect on the internal combustion engine" in Fuel Economy: Road Vehicles Powered by Spark Ignition Engines, Chapter 3, Ed.s: Hilliard, J.C. and Springer,G.S., Plenum Press, 1984

(19) Maly, R., Eighteenth Symposium (International) on Combustion, p.1747, Combustion Institute, 1981

(20) Ziegler, G.F.W., Maly, R.R. and Wagner, E.P., International
Conference on Combustion in Engineering, Vol.1, p.81, I.Mech. E., 1983
(21) Ziegler, G.F.W., Wagner, E.P., Saggau, B., Maly, R. and Herden, W., SAE Paper No. 840992, 1984
(22) H.M. Hertz and P. Thomsen, Rev. Sci. Instrum. 58 (9), September 1987
(23) Russo, Righini, Sottini, Trigari, Applied Optics, Vol.23, No.19, October 1984
(24) Spicher and Kollmeier, SAE Paper No. 861532, 1986
(25) Travers and Williams, Tenth Symposium (International) on Combustion, pp. 657-672, The Combustion Institute, 1965
(26) R. Carlsson and B. Johnsson, Diploma paper, LTH 1988
(27) Kono, Hatori, Tsukamoto and Niu, Recent Advances in Laser Diagnostics and Modelling of Combustion, Oct 1986
(28) M. Ackram, G. Holmstedt, L. Martinsson, IEA, Amalfi, Italy, 1988
(29) Kalghatgi, G., SAE Paper No. 870163, 1987

8 ADDITIONAL FIGURES & TABLES

Ion probe positioning (figure captions for fig.18)

a) The two probes were parallel to each other and to the spark-plug, pointing in the same direction and located on the same side of the spark-plug. The probe tips were at the same height as a spot 2 mm beyond the electrode center.

b) Same positioning as in a) but the probe tips were at the same height as the electrode centre.

c) Same positioning as in b) but the probes formed an angle of approximately 75 degrees to each other.

d) The two probes both pointed in the direction of the electrode centre but now formed an angle of 45 degrees to the spark-plug.

e) The two probe tips pointed at each other from opposite sides of the spark-plug, at the same height as the electrode center.

f) Same positioning as in d) but the probes were perpendicular to the spark-plug.

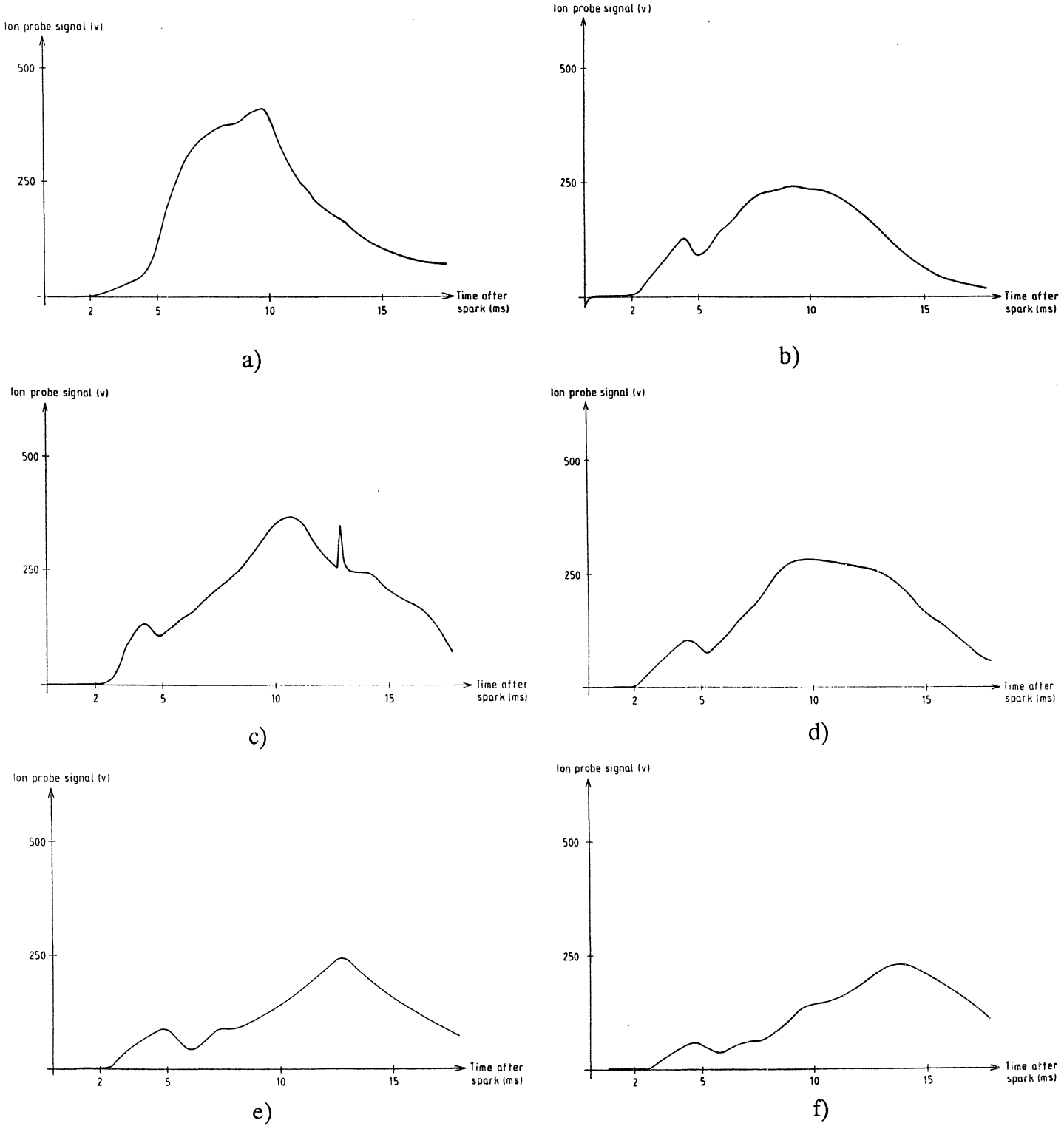

Fig.18 Signals from different geometries of the ion probe.

Tables of energies and propagation rates

Explanation of the symbols used: E=energy
v=propagation rate

Unless otherwise specified, the energy and the velocity were measured simultaneously.

Table 1
Ultra-fast system with the coaxial spark-plug.

E (mJ)	v (m/s)
49.2	5.0
55.1	5.8
67.9	6.0
71.8	6.0
77.4	6.2
89.1	6.7
94.4	6.0
99.9	6.0
103.1	4.9

Table 2
Ultra-fast system with the coaxial spark-plug.
The velocities are mean values ± 1 standard deviation.

E (mJ)	v (m/s)	
32.3	4.8±0.6	(8 shots)
55.7	5.5±0.6	(9)
64.0	5.2±0.8	(7)
75.6	6.1±0.6	(9)
88.2	5.1±0.7	(7)

Table 3
Ultra-fast system with the conventional spark-plug.
The velocities are mean values ± standard deviation from 6 shots.

E (mJ)			v (m/s)
0-1μs	0-10μs	0-100μs	
4.0	11	20	2.5±0.6
15.5	59	186	3.0±0.6

Table 4
Capacitive system with the conventional spark-plug. First part of the energy.

E (mJ)	v (m/s)
1.2	2.0
1.3	2.1
1.4	2.5
1.4	2.2
1.4	2.1
1.5	2.8
1.5	2.2

Table 5
Capacitive system with the coaxial spark-plug, 0.8 mm spark gap, first part of the energy. The last value is a mean value ± 1 standard deviation from 9 shots.

E (mJ)	v (m/s)
2.6	2.2
3.9	2.7
4.7	2.3
3.7	2.5 ± 0.2

Table 6
Capacitive system with the coaxial spark-plug, 1.05 mm spark gap, first part of the energy. Mean value ± 1 s.d.

E (mJ)	v (m/s)
2.9	2.7 ± 0.2

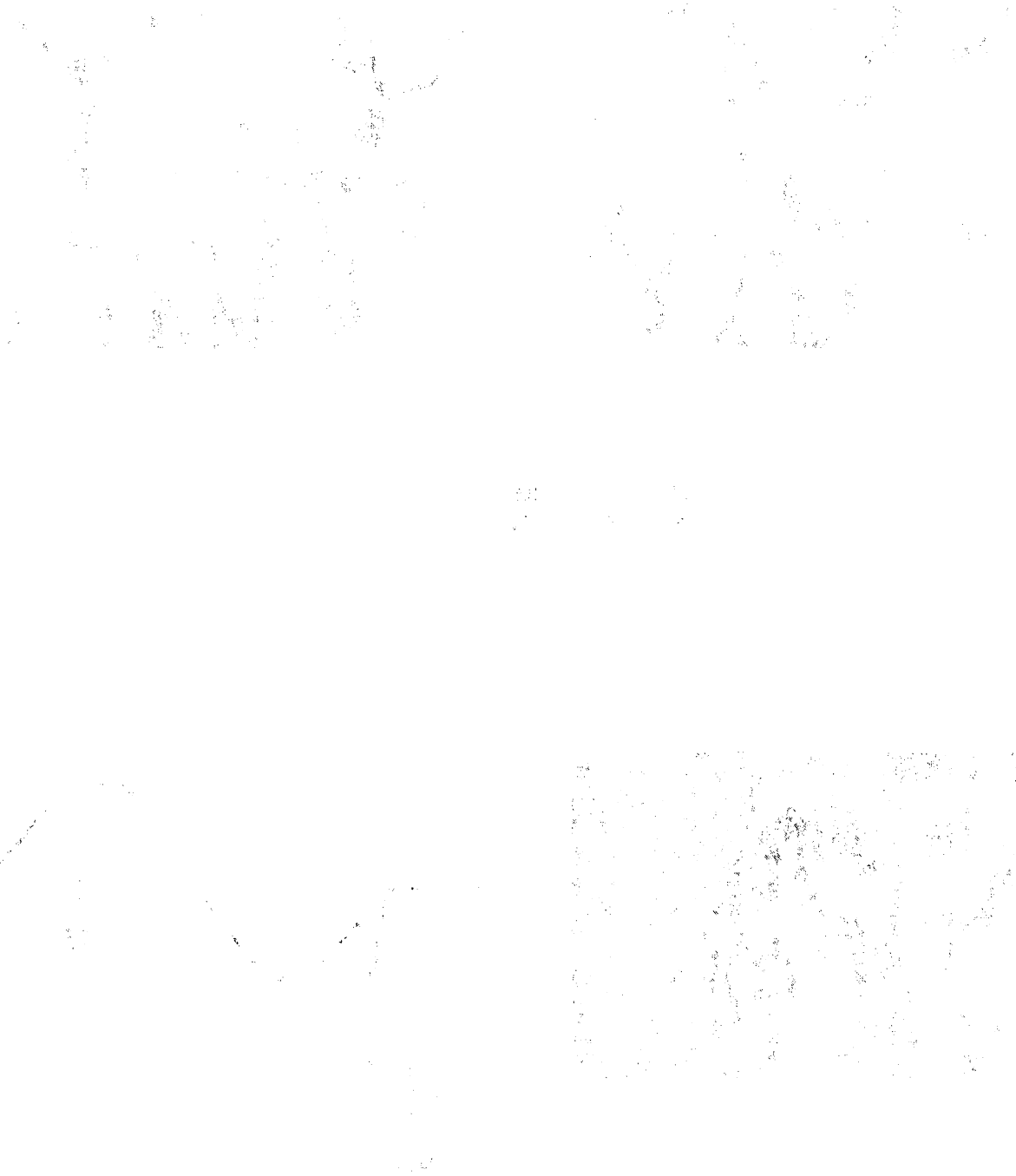

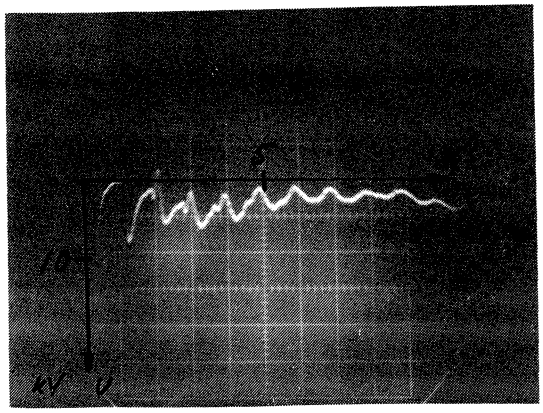

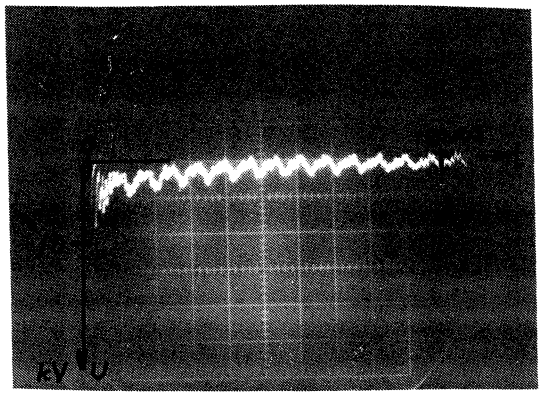

Ultra-fast system and
conventional spark-plug

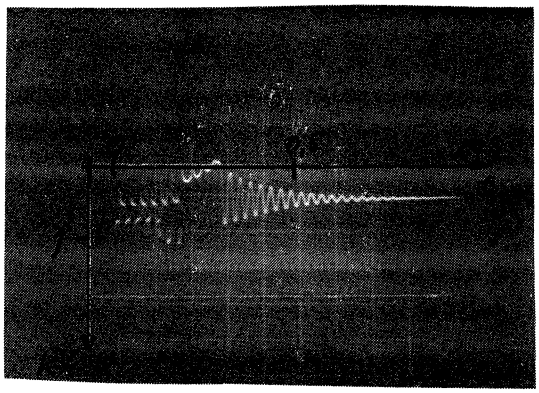

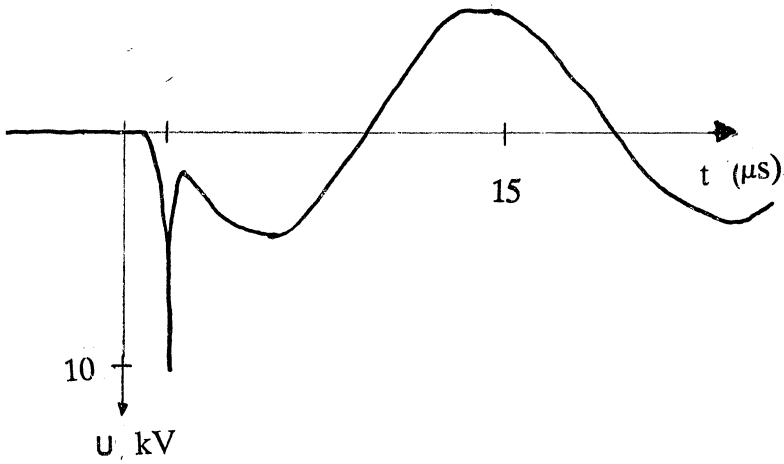

Capacitive system and
coaxial spark-plug

Capacitive system and
conventional spark-plug

Fig.19: Voltage characterization up to 100 μs

BARRACK LABORATORIES

Barrack Witze Probe

Barrack Laboratories, working in conjunction with Sandia National Laboratories, has developed the **Barrack Witze Probe™**, a unique optical device used for measuring the direction and rate of growth of early flame kernel development in spark ignition engines. This technology was first described by Peter O. Witze et al, of Sandia Labs. Barrack has continued the development and application of this probe. With **Barrack Witze Probe**, we can provide you with advanced technology for combustion research and analysis.

The **Barrack Witze Probe** is a set of eight fiber optic sensors. They are uniformly spaced in a ring within the base of the threaded region of a standard spark plug. This permits the use of the Probe in an unmodified production engine, greatly reducing the cost of analyzing common engine combustion problems.

The sensors are used to collect the light emitted from combustion as it crosses their field of view. These optical events are transmitted via fiber-optic cable to light detectors which are sensitive enough to detect the effects on flame kernel development caused by differences in the degree of residual gas scavenging and differences in swirl and turbulence levels. The fast electronics, developed to interface the probe with an on-line computer, allow measurements to be made on an individual cycle basis. This permits the investigation of the cause-and-effect relationships between early flame development and engine performance.

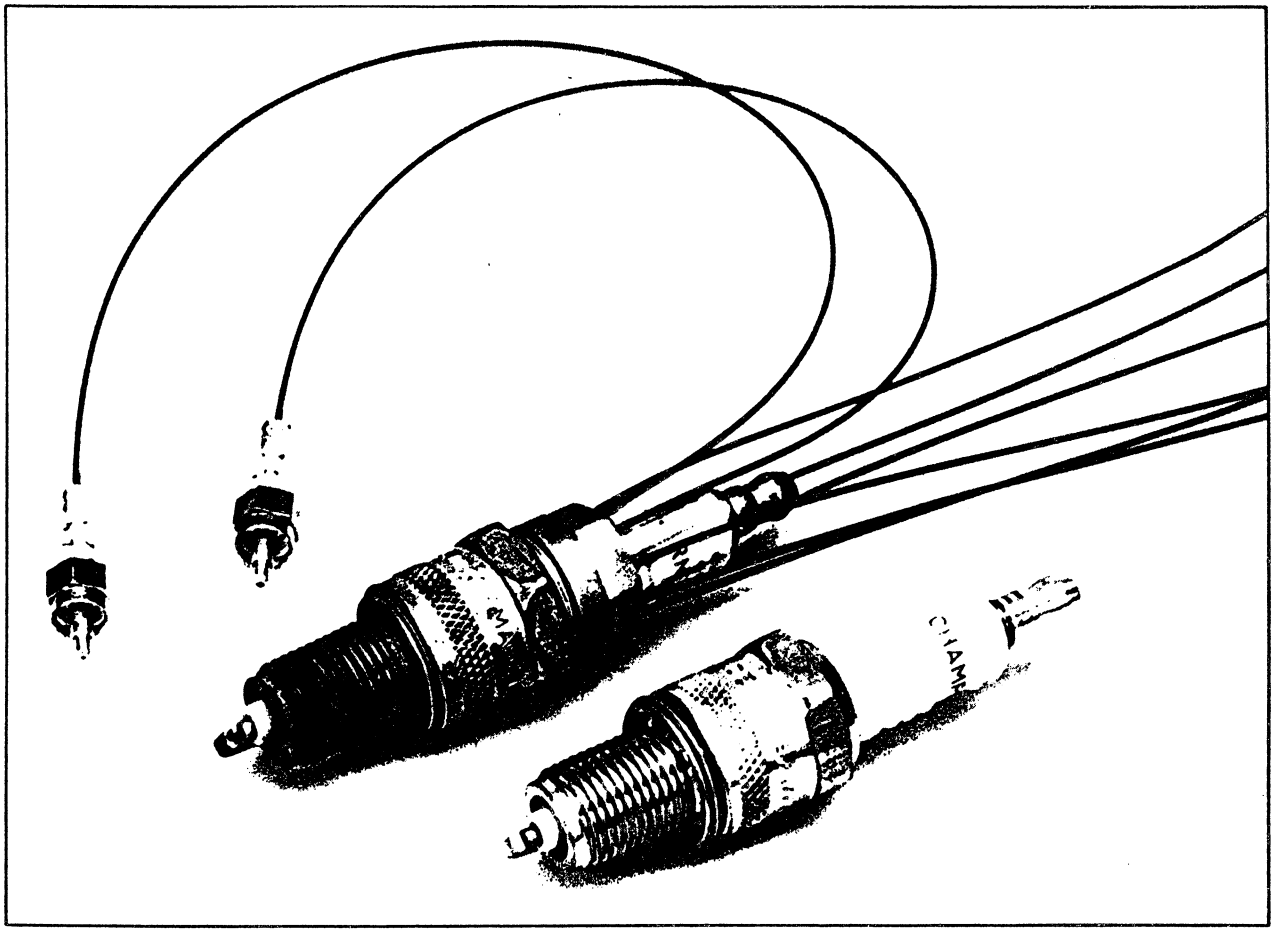

A modified automobile spark plug (left), together with a standard plug (right), has eight fiber—optic strands to see inside an engine. Result: a picture of the flame front early in the combustion cycle.

Fig.20: The commercial knock sensor